https://doi.org/10.15407/ufm.20.01.075

V.V. LIZUNOV, I.M. ZABOLOTNYY,
Ya.V. VASYLYK, I.E. GOLENTUS, and M.V. USHAKOV
G.V. Kurdyumov Institute for Metal Physics of the N.A.S. of Ukraine,
36 Academician Vernadsky Blvd., UA-03142 Kyiv, Ukraine

INTEGRATED DIFFRACTOMETRY: ACHIEVED PROGRESS AND NEW PERFORMANCE CAPABILITIES

This review provides a brief overview and a discussion of dynamical integrated diffractometry and its functional capabilities. It is demonstrated that the combined use of measurements of integrated diffraction parameters on different diffraction conditions allows determining the parameters of several types of microdefects, which are simultaneously present in a single crystal. These parameters are the total integrated intensity of dynamical diffraction, the contribution of its diffuse component, and their dependences on different diffraction conditions. Examples of the use of integrated diffraction parameters for non-destructive express diagnostics of the characteristics of the defects' structure of single crystals are discussed.

Keywords: dynamical diffraction, diffuse scattering, integrated diffractometry, microdefects.

1. Introduction

The development of materials with new, necessary for practical application properties, is often achieved by forming unique structural and phase states. It means that the corresponding advance of functional capabilities of the diagnostic equipment for controlling the structural perfection of the materials should be achieved. The diffractometry methods play the most important role in solve this problem and allow conducting non-destructive diagnostics of materials.

In addition, the important requirement (especially for practical applications) for diagnostic methods is short-term of the measurement. The reduction of the measurement time did the diagnostic method is more convenient, allowing more samples to be investigated for a fixed time.

© V.V. LIZUNOV, I.M. ZABOLOTNYY, Ya.V. VASYLYK, I.E. GOLENTUS, M.V. USHAKOV, 2019

Modern diffractometry methods chiefly use triple-axis and less commonly double-axis schemes. The use of triple-axis diffractometry makes possible to measure distributions of the diffracted radiation intensity in the reciprocal lattice space and, therefore, to determine the structure of the objects under study. However, with the advantages of the mentioned techniques, they also have disadvantages, which are long-term measurements, expensive radiation sources and complex equipment. Duration of the exposure time is associated primarily with problem of measuring too low values of the diffracted radiation intensity at each point of the reciprocal space. In other words, the problem is registration a small number of counts per unit time. An alternative to this would be to measure some integral parameters, which would increase the number of recorded counts per unit of time and thus significantly decrease the time of diagnostics. The development of similar integrated diffractometry methods began almost immediately after the discovery of the phenomenon of radiation diffraction on crystal structures about 100 years ago.

The first results were obtained for the integrated intensities, i.e. for the sum of intensities in all diffracted waves, including the energy distribution near the Bragg reflection. For describing the diffraction processes on crystals, the kinematical (single-scattering approximation) theory and rigorous dynamical theory (taking into account multiple scattering) were developed [1–6]. As a result, formulas that relate the magnitudes of the integrated intensities with the structural factors of the crystals were obtained. This allowed determining the structure of crystalline objects by simple non-destructive methods.

Most natural crystals are poly- and mosaic crystals, and no single crystals. So, for a long time there was a paradoxical situation: the formulas obtained within the framework of the approximate kinematical theory described the experiment much more accurately than the rigorous dynamical theory. Thus, the formulas of the kinematical theory of diffraction were sufficiently for the study of crystal structures. The effects of multiple scattering can be observed only when the coherence length of the scattering and the size of the crystals exceed the extinction length, *i.e.* in crystals close to perfect single crystals.

However, since 1960^s^, methods for growing almost perfect single crystals with a low concentration of microdefects have been developed. These crystals have been required in industry that stimulated a rapid growth in the number of studies related to dynamical diffraction.

In addition, later it found out that the properties of modern materials are determined not so much by the structure and parameters of their ideal periodic lattices, as by the statistical characteristics of the microdefects and parameters of substructure. Therefore, the theories of radiation diffraction on perfect crystals that existed at that time required generalization to the case of single crystals with microdefects.

A similar generalization was carried out in the works of M.A. Krivoglaz (systematic description of his results presents in the monographs [7, 8]), where a statistical averaging of the crystal susceptibility over the distribution of defects have been performed. As a result, periodical 'average' functions with new periods and effective atomic factors, as well as the fluctuation waves of deviations from this periodicity of the crystal susceptibility were introduced. In addition, relations between these new parameters and the characteristics of the defects were determined. As a result, the coherent (Bragg) and diffuse components of scattering radiation in the kinematical approximation were determined. Based on the obtained results, M.A. Krivoglaz classified microdefects according to their influence on the kinematical scattering pattern. Until today, Krivoglaz's classification is used in almost all structural laboratories in the world for characterizing crystals with microdefects.

However, the use of the kinematical theory of scattering for characterization of imperfect crystals significantly limited the applicability of the integrated intensities methods. As shown, the total (the Bragg + + diffuse components) integrated intensity does not depend on the distortion of the crystal lattice at kinematical diffraction. Thus, the methods for characterizing structure, based on measuring the total integrated scattering intensities, are inapplicable for kinematically scattering crystals with microdefects.

The situation changes due to the use of the dynamical scattering pattern instead of the kinematical one. It was shown that the dynamical pattern of scattering is sensitive to structure imperfections of crystals due to the dispersion mechanism. This mechanism also provides the sensitivity to structure imperfections in individual integral characteristics of scattering pattern (see, for example, [9, 10]). Thus, the measurement of the total integrated intensity of dynamical diffraction (TIIDD) allows quantifying the characteristics of the defect structure of single crystals.

In this article, we illustrate the use of dynamical diffraction methods to determine the parameters of structural imperfections of single crystals on examples of semiconductor materials. However, the appropriateness of using dynamical methods for characterization of metallic single crystals with microdefects is perhaps even higher than for semiconductors. The fact is that without taking into account the effects of dynamical scattering of radiation in metallic single crystals the description of the defect structure can be not only quantitatively but also qualitatively incorrect. For example, the kinematical description of single crystals with dislocations predicts a complete absence of a coherent component of intensity. At the same time, the use of the dynamical approach with taking into account the effects of multiple scattering leads to an effective cutoff of the contribution of distant dislocations to the scattering

characteristics. As a result, even at high concentration of dislocations in the crystal, coherent peaks can be preserved. The same scattering pattern is observed experimentally.

The article has following structure. In Section 2, some of the classical results of the integrated intensity theory for mosaic and perfect crystals are briefly described. In Section 3, the problems of the statistical scattering theories related with interpreting scattering patterns for crystals with several types of microdefects are presented. The main results of the statistical theory of TIIDD in crystals with microdefects, which allow solving these problems, are described in Section 4.

2. The Intensity of Integrated Reflection of X-Ray by Crystals

2.1. The Integrated Reflection from Mosaic Crystals

The majority of nature crystals are not single crystals. In fact, crystal which appeared one whole consists of a number of independent crystalline regions. Each such region is a small single crystal block in which the atomic planes are regular and parallel. The whole crystal consists in very large number of such blocks; their atomic planes are almost parallel, but the orientations are distributed in a certain range of angles, although small, but still larger than the angular region of reflection from a single block. Such composite crystals on the proposal of Ewald are called mosaic crystals.

For simplicity, we assume that the individual blocks are small enough and the absorption in them can be neglected. The intensity of the scattering radiation by a single crystal block is described by the expression [5, 11]:

$$J = \frac{|\Phi_0|^2}{R^2} I_0(\xi, \eta, \zeta), \tag{1}$$

where

$$I_0(\xi, \eta, \zeta) = \frac{\sin^2(\pi N_1 \xi)}{\sin^2(\pi\xi)} \frac{\sin^2(\pi N_2 \eta)}{\sin^2(\pi\eta)} \frac{\sin^2(\pi N_3 \zeta)}{\sin^2(\pi\zeta)} \tag{2}$$

is Laue interference function; Φ_0 is the amplitude of the scattered wave at unit distance from the scattering point (lattice-point); N_1, N_2, N_3 are the numbers of lattice-points in the block in the directions of the basis lattice vectors; ξ, η, ζ are the integers coordinates of the diffraction vector in reciprocal space, R is the distance from the crystal to the observation point.

For calculation the intensity scattered from the whole crystal it is necessary to sum the intensities scattered from each of the blocks. Since the blocks are disoriented, it is need to sum up exactly the intensities, not the amplitudes of the scattered waves.

The reflection intensity has a sufficiently large value in the small range of the incidence angles. The maximum value of the reflected intensity corresponds to the incident radiation by the Bragg angle θ_B. Usually, under measuring integrated reflections the crystal is rotated with a constant angular velocity ω around an axis parallel to the reflecting planes and perpendicular to the direction of incidence [11].

Let I is the total diffracted intensity recorded during crystal rotation over the entire reflection region and I_0 is the intensity of the incident beam, then I/I_0 is called the integrated reflection from the crystal element. As shown in [11]:

$$\rho = \frac{N^2\lambda^3}{\sin 2\theta_B}|F|^2\left(\frac{e^2}{mc^2}\right)\frac{1+\cos^2 2\theta_B}{2}\Delta v = Q\Delta v\,, \quad (3)$$

where Δv is the volume of the irradiated crystal element, N is the number of atoms per unit volume, F is the structural factor, λ is the radiation wavelength, e and m are the electron charge and mass, c is the speed of light. The parameter Q characterizes the scattering intensity by a unit volume of the crystal. Thus, the measurement of the integrated reflection allows determining the structural factor of the crystal, and, consequently, its atomic structure.

The scattering patterns from different blocks of the mosaic crystal displace relative to each other that lead to some blurring of the resulting scattering pattern. In addition, the finite size of the x-ray source also leads to a blurring of the measured scattering pattern. Thus, there is an additional appropriateness of measuring of the integrated intensity, since the redistribution of the scattered energy does not change its total value.

2.2. The Integrated Reflection from Perfect Crystals

Now we consider the scattering of radiation by perfect single crystals. In according the kinematical theory for calculating the intensity scattered by the whole crystal the intensities (not amplitudes) scattered by individual blocks are summed. Therefore, the calculation of the intensity is reduced to calculation of the intensity of the radiation scattered by one block. The amplitude of the wave scattered by one block is small compared with the amplitude of the incident wave, so the interaction between this waves can be neglected. However, when the size of the crystal is large and it is a single crystal, this statement becomes incorrect.

For x-rays, the ratio q of the amplitudes of a wave scattered by a single atomic plane to the amplitude of the incident wave is about 10^{-5}; so for a large number of atomic planes the amplitude of the scattered wave becomes comparable to the amplitude of the incident wave and its interaction cannot be neglected.

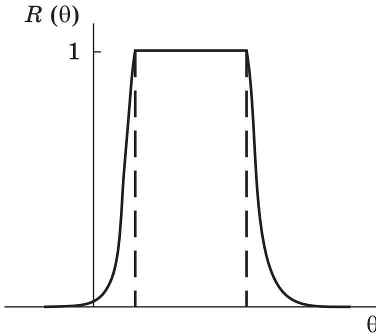

Fig. 1. Reflection curve of a perfect single crystal

Dynamical theory was developed in two forms: Darwin theory and Ewald–Laue theory. Darwin's dynamical theory was constructed by analogy with the kinematical theory. Each atom in the crystal lattice is characterized by an atomic scattering function, and waves scattered by atoms are added, taking into account the phases and scattering amplitudes. Darwin's theory takes into account the interaction of the crystal not only with the incident, but also with the scattered waves, as well as absorption. In the Ewald–Laue theory, the propagation of electromagnetic waves in a medium with taking into account the continuous distribution of electron density was considered.

Both of these approaches are equivalents, in whole, and in many cases give the same results. However, the Ewald–Laue theory was developed much more intensively because it allows solving a much wider range of problems. Here we present only formulas describing the integrated reflection from a perfect single crystal.

We consider a non-absorbing perfect single crystal. Let us note T_0 and S_0 the amplitudes of the incident and reflected waves. It was shown (see, e.g., [11]) that:

$$\frac{S_0}{T_0} = \frac{-q}{\varepsilon \pm \sqrt{\varepsilon^2 - q^2}}, \qquad (4)$$

where q determines the amplitude of the wave scattered by an atomic plane in the direction of the reflected beam, and ε is a small value connected with the deviation of the incidence angle of radiation θ from the exact Bragg angle.

The corresponding reflection curve is presented in Fig. 1. A characteristic property of this curve is the presence of a region of total reflection: in the interval $-q < \varepsilon < q$, the ratio $S_0/T_0 = 1$.

The integrated reflection will be determined by the area under the curve in Fig. 1:

$$\rho = \int_{-\infty}^{\infty} R(\theta) d\theta = \int_{-\infty}^{\infty} \left|S_0 / T_0\right|^2 d\theta. \qquad (5)$$

By the integration for nonpolarized radiation can be obtained [11]:

$$\rho_{\text{dyn}} = \frac{8}{3\pi} \frac{N\lambda^2}{\sin 2\theta_{\text{B}}} F(2\theta) \frac{1 + \left|\cos 2\theta_{\text{B}}\right|}{2}. \qquad (6)$$

This formula in essence is different from formula (3) for the integrated intensity of a mosaic crystal. It can be seen from formulas

 ISSN 1608-1021. Prog. Phys. Met., 2019, Vol. 20, No. 1

that $\rho_{kin} \sim \propto F^2$ and $\rho_{dyn} \propto F$. The difference between ρ_{dyn} and ρ_{kin} can reach 30–40 times, and the dynamical integrated intensity is less than kinematical despite the presence of a region of total reflection. One of the reasons for this is that the width of the reflection curve of perfect single crystal is very small (several angular seconds), and for a mosaic crystal the width of the reflection curve is much larger.

It should be noted that when radiation is incident on a crystal at the Bragg angle, only the upper layers of the crystal take part in the reflection. This is because the waves twice reflected from the crystal planes, which propagate in the direction of the primary wave, differ from the primary wave in phase by π and as a result, the primary wave is quickly extinguished. This phenomenon is called the primary extinction. The primary extinction can be formally interpreted as an effective increase of the absorption coefficient around the reflection region. In this angle range, the intensity of the incident beam is attenuated not only by ordinary absorption, but also by transfer to the reflected wave.

Formula (6) was obtained for an infinite single crystal. It is necessary to consider the interaction of radiation with a single crystal of finite size with correct boundary conditions for the practical use of integrated intensity.

If the blocks of the mosaic crystal are large enough, then it is necessary to take into account the extinction for each of them. The formula for a mosaic crystal with taking into account primary extinction can be written [1, 2]:

$$\rho = Q\Delta v \frac{\mathrm{th}(pq)}{pq}, \tag{7}$$

where p is the number of atomic crystal planes. This formula allows determining the size of coherent blocks in a mosaic crystal.

Thus, the use of integrated intensity methods allows determining the structural characteristics of ideal mosaic crystals, as well as perfect single crystals.

3. Integrated Intensity of Reflection for Crystals with Microdefects

Any real single crystal contains microdefects, the statistical characteristics of which determine its properties. For describing the radiation diffraction on single crystals with microdefects M. A. Krivoglaz created the statistical kinematical theory of scattering in the 1950s. This theory gives the following formulas for the total integrated intensity (TII) R_i [8, 17, 18]:

$$R_i = R_{iB} + R_{iD}, \tag{8}$$

$$R_{iB} = R_{ip} e^{-2L}, \tag{9}$$

$$R_{iD} = R_{ip}(1 - e^{-2L}), \quad (10)$$

$$R_{ip} = C^2 Qt/\gamma_0, \quad (11)$$

$$Q = (\pi|\chi_{Hr}|)^2/[\lambda\sin(2\theta_B)]. \quad (12)$$

Here R_{ip} is the integrated scattering intensity in the perfect crystals (without microdefects), χ_{Hr} is the real part of the Fourier component of the polarizability of the crystal, t is the crystal thickness, C is the polarization factor.

It should be noted that in expressions (9) and (10) for Bragg (R_{iB}) and diffuse (R_{iD}) components of TII, only the factor R_{ip} is dependent on diffraction conditions. In addition, factor R_{ip} does not depend on the defects structure of the crystal. Only the factors that include the Krivoglaz factor (static Debye–Waller factor $E = e^{-L}$) depend on the characteristics of the defects structure of crystal lattice. The Krivoglaz factor is independent on the diffraction conditions for each reflex.

From formulas (8)–(12), it follows that the integrated intensity in crystals with microdefects can be characterized by two integral parameters. The first parameter is the total brightness of the scattering pattern, i.e. the total integrated reflection intensity R_i, equal to the sum of the Bragg and diffuse components (see Eq. (9)). For convenience this parameter should be normalized to the total brightness of the scattering pattern of an perfect crystal (R_{ip}). The second parameter is the specific contribution of the diffuse component or the ratio of the diffuse and Bragg components (R_{iD}/R_{iB}). From formulas (8)–(12) it follows that in the kinematical theory of non-ideal crystals:

$$R_i = R_{ip} \text{ or } R_i/R_{ip} = 1, \quad (13)$$

$$R_{iD}/R_{iB} = (1 - e^{-2L})/e^{-2L} \approx 2L, \quad (14)$$

Thus, for fixed reflex the total integrated intensity does not depend on the distortions of the crystal lattice, and the only structurally sensitive factor is the second parameter (R_{iD}/R_{iB}), which is not depend on diffraction conditions.

From the expressions (13) and (14) two conservation laws of the kinematical theory is followed. The first conservation law is the independence of the total integrated intensity R_i from the characteristics of crystal defects. Therefore, in kinematical theory R_i for a crystal with defects remains the same as in a perfect crystal (R_{ip}) and depends only on diffraction conditions. However, the normalization of this parameter to R_{ip} leads to a loss of dependence on diffraction conditions and makes it a universal constant equal to unity in the kinematical theory, i.e. completely uninformative. The second law of conservation of the kinematical theory is the independence of the contribution of the diffuse component from the diffraction conditions for each reflex. Thus, in the

kinematical case, there is only this structurally sensitive parameter for any diffraction conditions. As a result, the use of integrated methods for kinematical scattering is practically meaningless.

The Kato's statistical dynamical theory of diffraction [19, 20] and its improved modifications [21–26] were also widely known. However, measurements for imperfect crystals showed a discrepancy between experimental data and Kato's theory. For example, in [27] the integrated intensity in the Bragg diffraction geometry for silicon crystals with defects was measured. It was found that in most cases Kato's theory does not correctly describe obtained experimental data. This is due to the fact that Kato's theory is based on solving the Takagi equations [28], which are valid only for smooth displacement fields. For this reason Kato's theory is generally not applicable or not sufficiently correct quantitatively for single crystals with microdefects.

In addition, this approximation is closely related with the concept of a single optical path in the scattering plane and does not allow to correctly describing the processes of multiple diffuse scattering near Bragg reflection, which also include waves with diffraction vectors beyond the coherent scattering plane. This disadvantage was noted in [24], in which calculations based on the Green function method in real space are given with taking into account the second derivative with respect to the spatial coordinate corresponding to the vertical divergence. Kato also noted this problem in Ref. [29], where his previous approximation [19, 20] was reformulated without using the Takagi approximation.

Another problem in mentioned statistical dynamical theories is that they are aimed at solving the problem of secondary extinction and are based on the imperfect crystal model, which consists of mosaic blocks. As a result, the formulas for the integrated diffraction intensity include as parameters of imperfection the Krivoglaz factor and correlation lengths, which are related, in particular, to the block sizes. However, correlation lengths cannot be directly associated with the characteristics of microdefects (concentration, radius, etc.) when considering the imperfect single crystals. Therefore, in this case a completely different problem should be solved and completely different methods.

4. Methods of Total Integrated Intensity of Dynamical Diffraction in Single Crystals with Microdefects

In the case of dynamical scattering both integral parameters, defined in the previous section, are depended on the characteristics of the defect crystal structure. This allows us to determine the parameters of the defect crystal structure by measuring the dependences of TIIDD on different diffraction conditions and their combined processing using the

formulas of Molodkin dynamical theory [12–18]. Methods based on this approach are express and have the highest sensitivity compared to other diffraction methods. Measurements can be made under all possible diffraction conditions (Laue and Bragg geometries, cases of 'thin' and 'thick' crystals, spectral, azimuthal, deformation dependencies, etc.). Let us consider these cases in more detail.

4.1. The Method of Thickness Dependences of TIIDD

One of the primary methods of TIIDD is the method of the measuring of thickness dependences [18, 30–36]. As shown, the diffracted integrated intensities are significantly depended on the crystal thickness and the radiation energy. Two limiting cases of dynamical diffraction exist. They correspond to the so-called approximations of 'thin' ($\mu_0 t < 1$) and 'thick' ($\mu_0 t >> 1$) crystals [17], where μ_0 is the coefficient of linear photoelectric absorption and t is the thickness of the crystal. The important advantage of this method, as well as others methods, based on the measurement of TIIDD, is the possibility of a significant increase of the diffuse component compared to the coherent component.

Figure 2 presents the results of an experimental measurement of the thickness dependence of the contribution of diffuse scattering and violation of the first conservation law. Markers show the experimentally

Impurities composition and conditions of heat treatment of samples of dislocation-free silicon

No.	Orientation of the large sample surface	Impurities composition	Conditions of heat treatment
1	Plane (110) parallel to the direction of growing ingot 001	O_2 — $8.2 \cdot 10^{17}$ cm^{-3} Ge — 10^{20} см$^{-3}$	Annealing for 2 hours at 1523 K in Ar atmosphere
2	—	O_2 — $8.2 \cdot 10^{17}$ cm^{-3} Ge — 10^{19} cm^{-3}	Annealing for 2 hours at 1523 K in Ar atmosphere
3	—	O_2 — $8.2 \cdot 10^{17}$ cm^{-3} Ge — 10^{20} cm^{-3}	Annealing for 2 hours at 1523 K in Ar atmosphere, Cu diffusion for 1 hour at 1173 K in N_2 atmosphere
4	—	O_2 — $8.2 \cdot 10^{17}$ cm^{-3} Ge — 10^{19} cm^{-3}	—
5	—	O_2 — $8.2 \cdot 10^{17}$ cm^{-3} Ge — 10^{20} cm^{-3}	Cu diffusion for 1 hour at 1173 K in N_2 atmosphere
6	—	O_2 — $8.2 \cdot 10^{17}$ cm^{-3} Ge — 10^{19} cm^{-3}	—
7	Plane (111) perpendicular to the direction of growth of the ingot 111	O_2 — $8.2 \cdot 10^{17}$ cm^{-3}	Cu diffusion for 3 hours at 1173 K in N_2 atmosphere

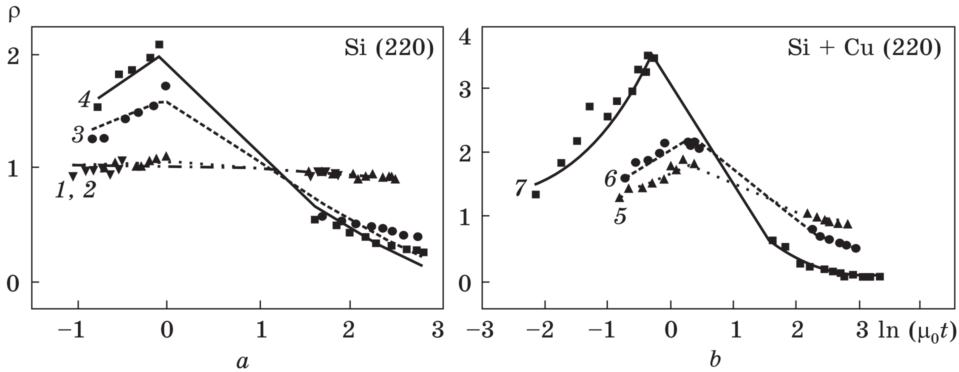

Fig. 2. TIIDD normalized to R_{ip} vs. value of $\mu_0 t$ for samples *1–4* (*a*) and *5–7* (*b*), the heat treatment conditions are listed in Table

measured thickness dependences of TIIDD, and the solid lines show the results of theoretical calculations.

Samples were cut from Si ingot without dislocations, grown by the Czochralski method (see Table). TIIDD were determined using a uniaxial diffractometer for symmetric (220) Laue reflexes using FeK_α-, CuK_α- and MoK_α-radiation. The thickness of the samples was varied by bleeding from 1000 to 300 μm. For FeK_α- and CuK_α-radiations the approximation of 'thick' crystal was realized and for MoK_α-radiation the approximation of 'thin' crystal was realized.

According to the kinematical theory, the ratio $\rho = R_i/R_{ip}$ should be a constant equal to unity in all range of $\mu_0 t$, regardless of the degree of distortion of the crystal lattice.

As can see, the deviations of the real experimental dependencies from the kinematical line ($\rho = 1$) are an order of magnitude greater than the experimental error (~10%) even for weakly disturbed single crystals. The deviations sharply increase with increasing degree of distortion of the crystals, demonstrating a high sensitivity of the proposed method.

It should be noted that, in accordance with the developed physical concepts [17, 30], the obtained curves deviate from the kinematical line in opposite directions in approximations of 'thin' and 'thick' crystals. A change in the heat treatment conditions leads to a change in the defect structure of the crystals under study and, accordingly, to a significant difference in the thickness dependences of TIIDD among themselves. Thus, the use of the thickness dependence method allows us to determine the parameters of the defect structure of a single crystals.

4.2. The Method of Energy-Dispersion Dependences of TIIDD

The method of the energy-dispersion dependences of TIIDD is closely related with the method of the thickness dependences of TIIDD. The difference of the method of the energy-dispersion dependences is changing the effective thickness of the crystal by changing the wavelength.

In the work [37], TIIDD were measured for different wavelengths and reflexes from dislocation-free Si single crystals of varying degrees of structural perfection. Samples of dislocation-free silicon single crystals were cut from Czochralski-grown ingot (p-type conductivity, $\rho \sim 10$ Ohm/cm, the growth axis was directed along the $\langle 111 \rangle$, oxygen and carbon concentrations were $1 \cdot 10^{18}$ cm^{-3} and 10^{16} cm^{-3}, respectively). The samples were prepared in the form of plates parallel to the (111) plane, which made an angle $\psi = (2.0 \pm 0.1)°$ with the surface. Disruptions of the surface structure because of mechanical processing were removed by chemical-mechanical polishing and next chemical etching to a depth of ~10 μm. Samples no. 1 and no. 2 were annealed in air and sample no. 3 was annealed in a nitrogen atmosphere for 4, 6, and 7 hours at 1000 °C, 1080 °C, and 1250 °C, respectively. Sample thicknesses were controlled with an accuracy of 1 μm and were equal to 490 μm, 488 μm, and 487 μm for samples nos. 1, 2 and 3, respectively.

Figure 3 shows the spectral dependences of TIIDD for mentioned non-ideal crystals, which are experimental confirmation of the difference between dependences of TIIDD in the approximations of 'thin' and 'thick' crystals in the case of Bragg diffraction.

As follows from the presented results, in the considered case the high sensitivity of the dynamical scattering pattern to the defect structure of single crystals is observed.

4.3. The Method of Azimuthal Dependences of TIIDD

It was considered that the azimuthal dependences (AD) of the normalized TIIDD for different types of lattice distortions are symmetric about an angle of 90°. For study the mentioned symmetry of AD were measured for a crystal with defects (see Refs. [31, 32, 38]). The objects of study were the same as described in the previous section. The sample was made in the form of a plate parallel to the (111) plane, with a thickness of t = 4000 μm. Disruptions of the surface structure because of mechanical processing were removed by chemical-mechanical polishing and next chemical etching to a depth of ~10 μm.

It was experimentally established that as a result of the presence of large-size defects in this crystal (dislocation loops with a radius of 15 μm) AD of the normalized TIIDD is asymmetric (see Fig. 4, *a*, markers). The calculation also gives the asymmetry of AD of the normalized TIIDD and practically coincides with the experiment (Fig. 4, *a*, solid line).

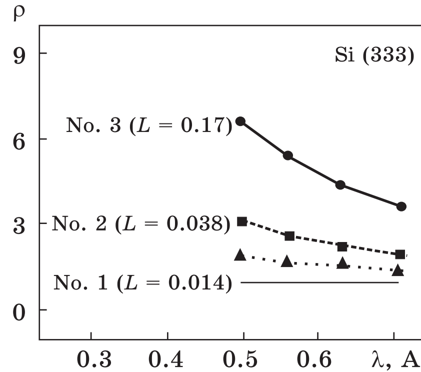

Fig. 3. TIIDD normalized to R_{ip} vs. radiation wavelength for single crystals Si with microdefects in the case of Bragg diffraction geometry. The results of the calculation show solid lines, the experiment show markers

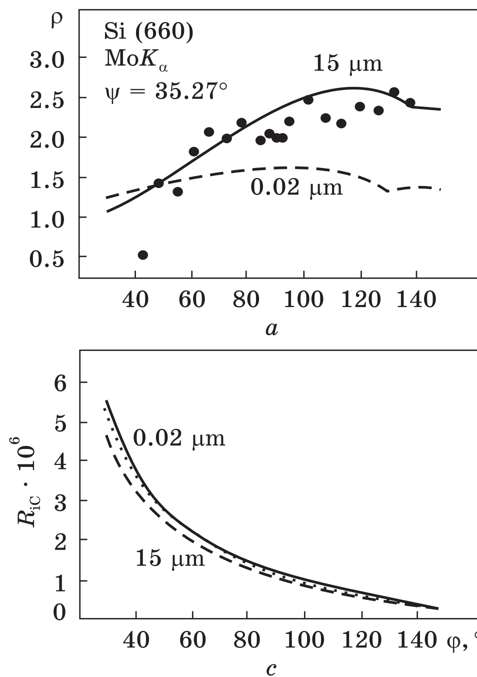

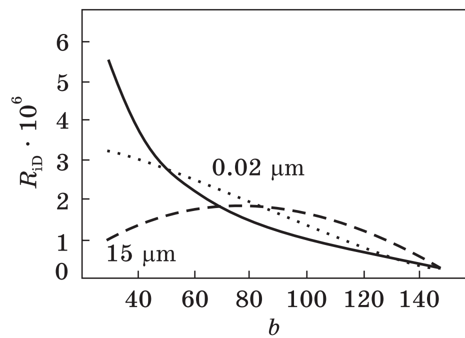

Fig. 4. Experimental (markers) and calculated AD of TIIDD at the values of the average radius of the dislocation loops R = 15 μm (solid line) and R = 0.02 μm (dash line) (*a*); the calculated AD of TIIDD for an ideal crystal (solid line) as well as the calculated AD of diffuse component of TIIDD R_{iD} (*b*) and coherent components of TIIDD R_{iC} (dashed and dotted lines) (*c*)

Analysis of the causes of the asymmetry of AD showed that this effect is explained by the behaviour of the diffuse component of TIIDD. It has been established that the presence of large-sized defects in a single crystal causes the symmetry of non-normalized diffuse component of AD (which asymmetric in the case of small defects), while AD of coherent component remains asymmetric (as in the case of a perfect crystal). It is shown in Figs. 4, *b*, *c*.

Thus, by normalizing AD of TIIDD of single crystal with defects on similar AD of perfect crystal, we obtain a symmetric dependence in the case of small defects and asymmetric in the case of large defects. Thus, due to the different character of AD in cases of small and large defects,

and selective sensitivity of AD to large defects, it becomes possible to determine their parameters. The parameters of small defects can be determined using other diffraction conditions for the same sample.

4.4. The Method of Deformation Dependences (DD) of TIIDD

The methods of TIIDD described in the previous sections have disadvantages: when using the method of thickness dependences, it is not always possible to conserve the integrity of the original sample, and for all three methods it is impossible to exclude stochastic crystal deformations that influence to the measurement results. Research of the effect of macroscopic elastic deformation on the TIIDD not only made it possible to control its influence, but also formed the method for diagnostics of microdefects [18, 31–35, 39–42].

Figure 5 illustrates a significant change of the character of the defects effect on the integrated scattering intensity (first parameter)

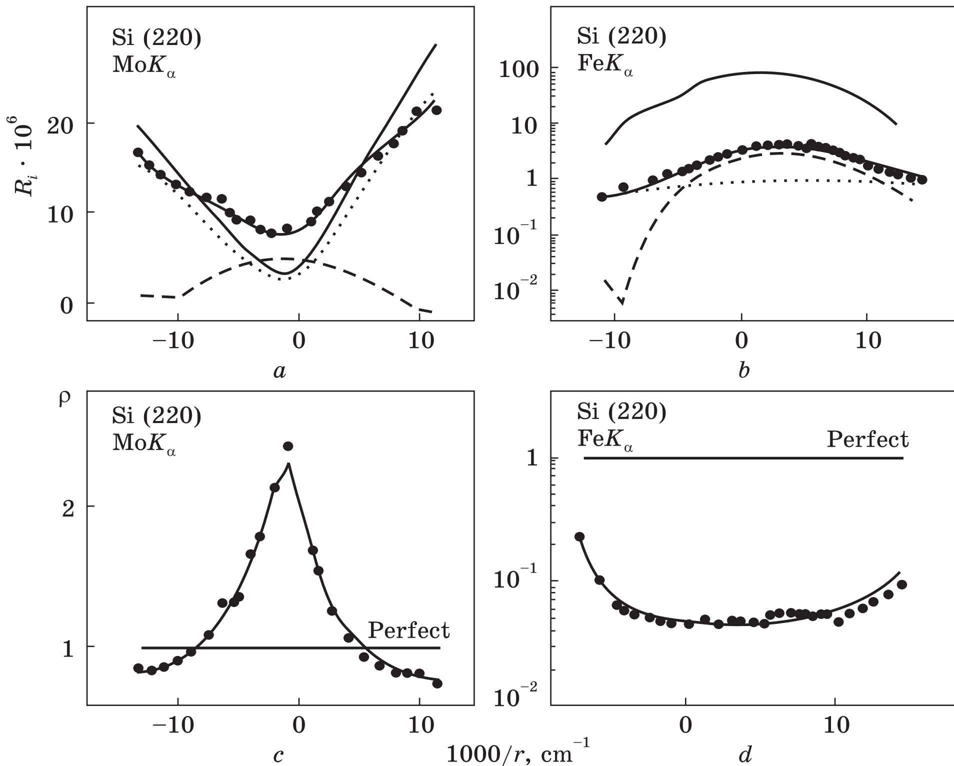

Fig. 5. Theoretical and experimental values of DD of TIIDD (*a* is a ‘thin’ crystal, *b* is a ‘thick’ crystal) and normalized DD of TIIDD (*c* is a ‘thin’ crystal, *d* is a ‘thick’ crystal) are shown with solid lines and markers, respectively. The dashed lines are the calculated DD of the coherent component of TIIDD, the dashed lines are the diffuse component, and the solid thin lines are DD of TIIDD crystal without defects

 ISSN 1608-1021. Prog. Phys. Met., 2019, Vol. 20, No. 1

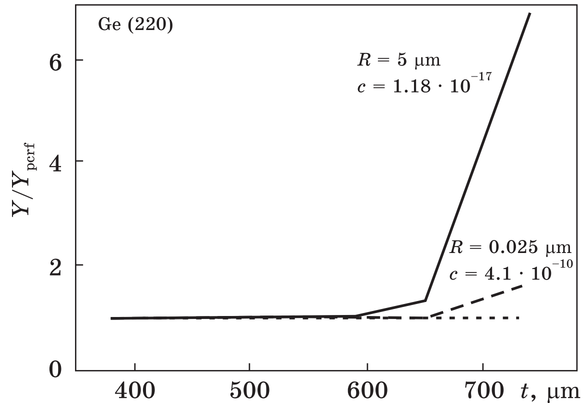

Fig. 6. The ratio of the change of parameter Y of a real Ge single crystal (the parameters of defects are shown in the figure) to the change of the parameter of an ideal perfect crystal vs. the thickness of crystal. The calculations were performed with the radius of curvature of the elastic bend $r = \pm 2.4$ m

depending on the radius r of curvature of the macroscopic elastic bending of a silicon crystal, as well as the change of the character of the defects effect on these DD depending on other diffraction conditions. Figure 5 shows mentioned change at the transition from the case of a 'thin' crystal (*a*) to the case of a 'thick' crystal (*b*). The total brightness of the dynamical scattering pattern, normalized to the brightness of the pattern for the perfect crystal, and its DD become sensitive to the characteristics of the defects.

In the next papers [43, 44], the use of DD of TIIDD to determine the parameters of the defect structure of silicon crystals with thicknesses significantly smaller than the absorption length and containing a relatively small number of defects was considered. In this case, the diffuse component has a small value and, accordingly, small value has the effect of its anomalous growth. In the work [45], the diagnostic capabilities of the method of DD of TIIDD for single crystals containing a larger number of defects were experimentally considered. In this case, the diffuse component of TIIDD is commensurate with its coherent component or significantly exceeds it. It was shown that in such cases DD of TIIDD are sensitive to the characteristics of microdefects in single crystals.

4.5. The Method of DD of TIIDD at Violation of the Friedel Law

This method is based on the influence of the defect structure of the crystal on the ratio of TIIDD for reflections (hkl) and $\overline{hkl}$: $Y = I^{hkl} / I^{\overline{hkl}}$. For example, the change of Y at the K-absorption edge is sensitive to large defects [46]. As can be seen from Fig. 6, for a crystal with defects, due to the contribution of the diffuse component, the thickness dependence of Y is different from the similar dependence for a perfect crystal. The characteristics of defects can be determined by the degree of this difference. Similarly, it is possible to determine via deviations of

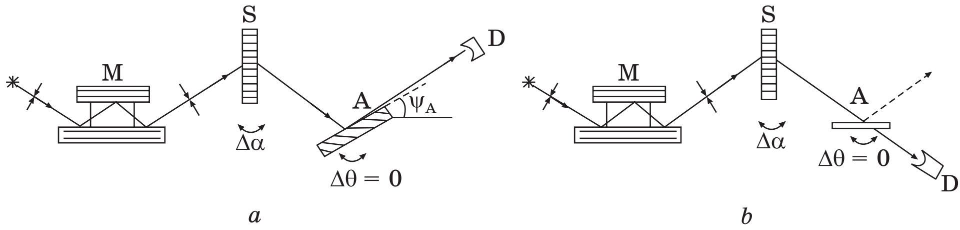

Fig. 7. The methods of separation of coherent (*a*) and diffuse (*b*) components of the total integrated intensity. Here M is a slit monochromator with three consecutive reflections, S is a sample crystal, A is an analyzer crystal, D is a detector

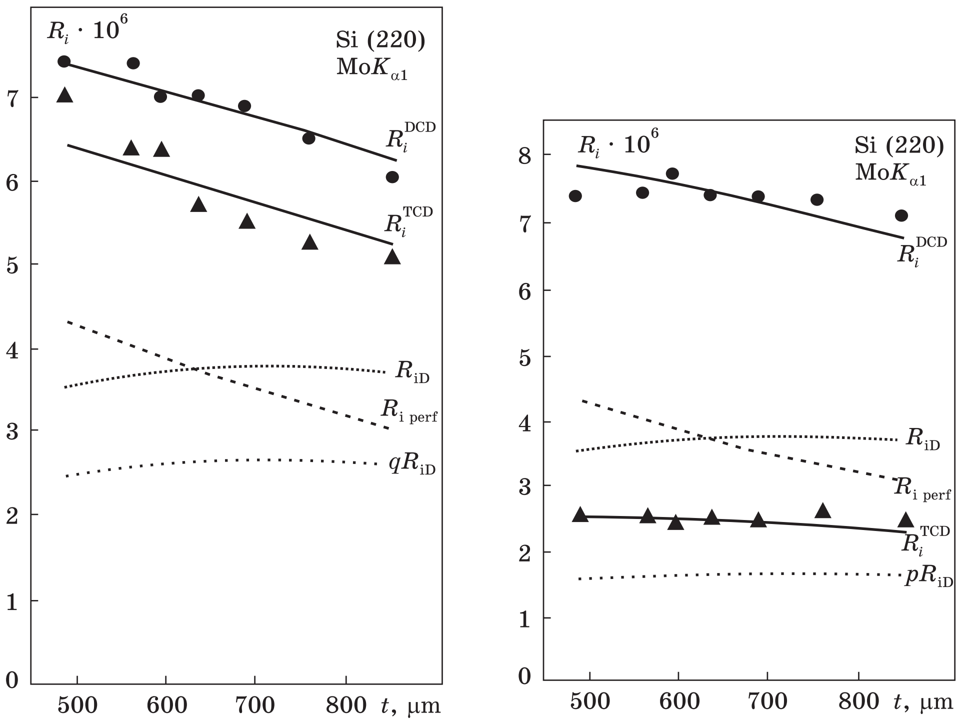

Fig. 8. Thickness dependences of TIIDD (•) and its coherent component (▲), measured by the slope method. Here solid lines are the result of theoretical calculations for the determined defects parameters, dashed line is the calculations for an ideal crystal, dash-dotted line is the separated true values of the diffuse component of TIIDD, and dotted line is the contribution of the diffuse component in the measured coherent component

Fig. 9. Thickness dependences of TIIDD (•) and its duffuse component (▲), measured by the slope method. Here solid lines are the result of theoretical calculations for the determined defects parameters, dashed line is the lost part of the diffuse component, dotted line is the calculations for an ideal crystal, and dash-dotted line is the separated true values of the diffuse component of TIIDD

the parameter Y for a single crystal with defects from the parameter Y_{perf} for a perfect crystal and their variations with thickness, both below and above the K-absorption edge.

4.6. The Method of Integrated Triple-Axis Diffractometry

In addition to measuring the dependences of the TIIDD (the first parameter) on diffraction conditions, similar dependences of the relative contribution of the diffuse component of the TIIDD (the second parameter) can be measured [47–49]. The scheme that is used is shown in Fig. 7.

Experimental measurements were carried out on a sample of Si cut along (111) surface perpendicular to the growth axis from an ingot grown according to Czochralski. A *p*-type conductivity sample (alloying element B, $\rho = 10\ \Omega \cdot cm$) with an oxygen atom concentration of about $1.1 \cdot 10^{18}$ cm^{-3} and carbon atoms 10^{16} cm^{-3} was heat treated in air at 1080 °C for 6 hours.

The experimental results of diagnostics using the method of integral triple-axis diffractometry [47–49] are presented in Figs. 8 and 9. The method of separation of the true contribution of the diffuse component developed in [48] was used.

Thus, the proposed measuring method makes it possible to increase the accuracy of determining the second structurally sensitive integrated parameter in comparison with the conventional methods. In addition, it should be noted that the redistributing of the contributions of the coherent and diffuse components to the measured intensity is feasible. This effect can be obtained by a choice of the width of the total reflection region of the analyzer crystal due to the asymmetry parameter or the reflection order. The redistribution can provide an optimization of measurements with respect to sensitivity to parameters of structural perfection, which affect the coherent and diffuse components of diffraction intensity in different ways.

5. Conclusions

The integrated diffractometric methods have a long and difficult history. For a long time the integrated reflectivity was the main measured parameter in most experiments for determination of the structural parameters of crystalline materials. However, since the 1980s the integrated methods were practically refused by the scientific community as uninformative and, therefore, useless in practice. However, the measurement of the total integrated intensity of dynamical diffraction can be extremely useful for determining the parameters of microdefects of several types that can simultaneously be in a single crystal. At the same time, the loss of informativity is compensated by the combined use of different dif-

fraction conditions and different methods, if they provide experimental measurements of both main integrated parameters of the dynamical scattering pattern (i.e., measurements of the corresponding parameters for both the full scattering pattern and its diffuse component) for the same sample. This approach may allow us to solve the problem of multi-parameterical diagnostics of single-crystal systems with microdefects.

Acknowledgements. The authors are grateful to the Corresponding Member of the National Academy of Sciences of Ukraine V. B. Molodkin for the support in their work and useful discussion of the article. This paper was supported by the National Academy of Sciences of Ukraine (contract no. 43Г/51-18).

REFERENCES

1. C.G. Darwin, *Phil. Mag.*, **27**: 315 (1914).
2. C.G. Darwin, *Phil. Mag.*, **27**: 675 (1914).
3. A.H. Compton, *Phys. Rev.*, **9**: 29 (1917). https://doi.org/10.1103/PhysRev.9.29
4. W.L. Bragg, R. W. James, and C.H. Bosanquet, *Phil. Mag.*, **41**: 309 (1921).
5. W. Friedrich, P. Knipping, and M. von Laue, *Sitzungsberichte der Kgl. Bayer. Akad. Der Wiss.*: 303 (1912); reprinted *Ann. Phys.*, **41**: 971 (1913).
6. M. von Laue, Sitzungsberichte der Kgl. Bayer. Akad. Der Wiss.: 363 (1912); reprinted *Ann. Phys.*, **41**: 989 (1913).
7. M.A. Krivoglaz, *Teoriya Rasseyaniya Rentgenovskikh Luchey i Teplovykh Neytronov Real'nymi Kristallami* [Theory of X-Ray and Thermal Neutrons Scattering by Nonideal Crystals] (Moscow: Nauka: 1967) (in Russian).
8. M.A. Krivoglaz, *X-Ray and Neutron Diffraction in Nonideal Crystals* (Berlin, Heidelberg: Springer-Verlag: 1996). https://doi.org/10.1007/978-3-642-74291-0
9. V.V. Lizunov, V.B. Molodkin, S.V. Lizunova, N.G. Tolmachev, E.S. Skakunova, S.V. Dmitriev, B.V. Sheludchenko, S.M. Brovchuk, L.N. Skapa, R.V. Lekhnyak, and E.V. Fuzik, *Metallofiz. Noveishie Tekhnol.*, **36**, No. 7: 857 (2014) (in Russian). https://doi.org/10.15407/mfint.36.07.0857
10. L.N. Skapa, V.V. Lizunov, V.B. Molodkin, E.G. Len', B.V. Sheludchenko, S.V. Lizunova, E.S. Skakunova, N.G. Tolmachev, S.V. Dmitriev, R.V. Lekhnyak, G.O. Velikhovskiy, V.V. Molodkin, I.N. Zabolotnyy, E.V. Fuzik, and O.P. Vas'kevich, *Metallofiz. Noveishie Tekhnol.*, **37**, No. 11: 1567 (2015) (in Russian). https://doi.org/10.15407/mfint.37.11.1567
11. R.W. James, *The Optical Principles of the Diffraction of X-Ray* (London: 1950).
12. V.B. Molodkin and E.A. Tikhonova, *Fiz. Met. Metalloved.*, **24**, No. 3: 385 (1967) (in Russian).
13. V.B. Molodkin, *Fiz. Met. Metalloved.*, **25**, No. 3: 410 (1968) (in Russian).
14. V.B. Molodkin, *Fiz. Met. Metalloved.*, **27**, No. 4: 582 (1969) (in Russian).
15. V.B. Molodkin, *Metallofizika*, **2**, No. 1: 3 (1980) (in Russian).
16. V.B. Molodkin, *Phys. Metals*, **3**: 615 (1981).
17. L.I. Datsenko, V.B. Molodkin, and M.E. Osinovskiy, *Dinamicheskoe Rasseyanie Rentgenovskikh Luchey Real'nymi Kristallami* [Dynamical X-Ray Scattering of Nonideal Crystals] (Kyiv: Naukova Dumka: 1988) (in Russian).
18. V.B Molodkin, A.I. Nizkova, A.P. Shpak, V.F. Machulin, V.P. Klad'ko, I.V. Prokopenko, R.N. Kyutt, E.N. Kislovskiy, S.I. Olikhovskiy, E.V. Pervak, I.M. Fodchuk, A.A. Dyshekov, and Yu.P. Khapachev, *Difraktometriya Nanorazmernykh*

Defektov i Geterosloev Kristallov [Diffractometry of Nanoscale Defects and Heterogeneous Layers of Crystals] (Kyiv: Akademperiodika: 2005) (in Russian).
19. N. Kato, *Acta Crystallogr. A*, **36**: 763 (1980). https://doi.org/10.1107/S0567739480001544
20. N. Kato, *Acta Crystallogr. A*, **36**: 770 (1980). https://doi.org/10.1107/S0567739480001556
21. M. Al Haddad and P. Becker, *Acta Crystallogr. A*, **44**: 262 (1988). https://doi.org/10.1107/S0108767387011681
22. P. Becker and M. Al Haddad, *Acta Crystallogr. A*, **45**: 333 (1989). https://doi.org/10.1107/S0108767388014692
23. P. Becker and M. Al Haddad, *Acta Crystallogr. A*, **48**: 121 (1992). https://doi.org/10.1107/S0108767391009376
24. A.M. Polyakov, F.N. Chukhovskiy, and D.I. Piskunov, *ZhETF*, **99**, No. 2: 589 (1991) (in Russian).
25. J.P. Guigay and F.N. Chukhovskii, *Acta Crystallogr. A*, **48**: 819 (1992). https://doi.org/10.1107/S0108767392003830
26. J.P. Guigay and F.N. Chukhovskii, *Acta Crystallogr. A*, **51**: 288 (1995). https://doi.org/10.1107/S0108767394010895
27. J.R. Schneider, H.A. Graf, and O. Goncalves, *J. Crystal Growth*, 80: 225 (1987). https://doi.org/10.1016/0022-0248(87)90067-4
28. S. Takagi, *Acta Crystallogr.*, **15**, No. 12: 1311 (1962). https://doi.org/10.1107/S0365110X62003473
29. N. Kato, *Acta Crystallogr. A*, **47**: 1 (1991). https://doi.org/10.1107/S0108767390008790
30. V.V. Nemoshkalenko, V.B. Molodkin, S.I. Olikhovskii, M.V. Kovalchuk, Yu.M. Litvinov, E.N. Kislovskii, and A.I. Nizkova, *Nucl. Instr. Phys. Res. A*, **308**, Nos. 1–2: 294 (1991). https://doi.org/10.1016/0168-9002(91)90651-6
31. A.P. Shpak, M.V. Koval'chuk, I.M. Karnaukhov, V.V. Molodkin, E.G. Len, A.I. Nizkova, S.I. Olikhovskiy, B.V. Sheludchenko, G.E. Ice, and R.I. Barabash, *Usp. Fiz. Met.*, **9**, No. 3: 305 (2008) (in Russian). https://doi.org/10.15407/ufm.09.03.305
32. A.P. Shpak, M.V. Koval'chuk, V.B. Molodkin, V.L. Nosik, S.V. Dmitriev, E.G. Len, S.I. Olikhovskiy, A.I. Nizkova, V.V. Molodkin, E.V. Pervak, A.A. Katasonov, L.I. Ninichuk, and A.V. Mel'nik, *Usp. Fiz. Met.*, **10**, No. 3: 229 (2009) (in Russian). https://doi.org/10.15407/ufm.10.03.229
33. A.P. Shpak, M.V. Koval'chuk, V.L. Nosik, V.B. Molodkin, V.F. Machulin, I.M. Karnaukhov, V.V. Molodkin, E.G. Len, G.E. Ice, R.I. Barabash, and E.V. Pervak, *Metallofiz. Noveishie Tekhnol.*, **31**, No. 5: 615 (2009) (in Russian).
34. A.P. Shpak, M.V. Koval'chuk, V.B. Molodkin, A.I. Nizkova, I.V. Hin'ko, S.I. Olikhovskiy, E.N. Kislovskii, E.G. Len, A.O. Bilots'ka, K.V. Pervak, and V.V. Molodkin, *Sposib Bahatoparametrychnoyi Strukturnoyi Diahnostyky Monokrystaliv z Dekil'koma Typamy Defektiv* [Method of Multiparameterical Structural Diagnostics of Single Crystals with Several Types of Sefects], Patent of Ukraine No. 36075 (Published October, 2008) (in Ukrainian).
35. A.P. Shpak, M.V. Koval'chuk, V.B. Molodkin, V.L. Nosik, V.Yu. Storizhko, L.A. Bulavin, I.M. Karnaukhov, R.I. Barabash, G.E. Ice, A.I. Nizkova, I.V. Hin'ko, S.I. Olikhovskiy, E.N. Kislovskii, V.A. Tatarenko, E.G. Len, A.O. Bilots'ka, K.V. Pervak, and V.V. Molodkin, *Sposib Bahatoparametrychnoyi Strukturnoyi Diahnostyky Monokrystaliv z Dekil'koma Typamy Defektiv* [Method of Multiparameterical Structural Diagnostics of Single Crystals with Several Types of Sefects], Patent of Ukraine No. 89594 (Published February, 2010) (in Ukrainian).

36. V.V. Nemoshkalenko, V.B. Molodkin, A.I. Nizkova, S.I. Olikhovskiy, A.P. Shpak, M.T. Kogut, and O.L. Shkol'nikov, *Metallofizika*, **14**, No. 8: 79 (1992) (in Russian).
37. V.V. Nemoshkalenko, V.B. Molodkin, E.N. Kislovskii, M.T. Kogut, A.I. Nizkova, E.N. Gavrilova, S.I. Olikhovskii, and O.V. Sul'zhenko, *Metallofiz. Noveishie Tekhnol.*, 16, № 2: 48 (1994).
38. V.B. Molodkin, S.V. Dmitriev, E.V. Pervak, A.A. Belotskaya, A.I. Nizkova, and A.V. Mel'nik, *Metallofiz. Noveishie Tekhnol.*, **28**, No. 8: 1055 (2006) (in Russian).
39. A.P. Shpak, V.B. Molodkin, S.V. Dmitriev, E.V. Pervak, I.I. Rudnitskaya, Yu.A. Dinaev, A.I. Nizkova, E.G. Len, A.A. Belotskaya, A.I. Grankina, M.T. Kogut, O.S. Kononenko, A.A. Katasonov, I.N. Zabolotnyy, Ya.V. Vasilik, L.I. Ninichuk, and I.V. Prokopenko, *Metallofiz. Noveishie Tekhnol.*, **30**, No. 7: 873 (2008) (in Russian).
40. A.P. Shpak, V.B. Molodkin, S.V. Dmitriev, E.V. Pervak, E.G. Len, A.A. Belotskaya, Ya.V. Vasilik, A.I. Grankina, I.N. Zabolotnyy, A.A. Katasonov, M.T. Kogut, O.S. Kononenko, V.V. Molodkin, A.I. Nizkova, L.I. Ninichuk, I.V. Prokopenko, and I.I. Rudnitskaya, *Metallofiz. Noveishie Tekhnol.*, **30**, No. 9: 1189 (2008) (in Russian).
41. A.N. Bagov, Yu.A. Dinaev, A.A. Dyshekov, T.I. Oranova, Yu.P. Khapachev, R.N. Kyutt, E.G. Len, V.V. Molodkin, A.I. Nizkova, A.P. Shpak, and V.A. Elyukhin, *Rentgenodifraktsionnaya Diagnostika Uprugo-Napryazhennogo Sostoyaniya Nanogeterostruktur* [X-Ray Diffraction Diagnostics of the Elastic-Stressed State of Heterogeneous Nanostructures] (Eds. B. S. Karamurzov and Yu. P. Khapachev) (Nal'chik: Kabardino-Balkarskiy Universitet: 2008) (in Russian).
42. A.P. Shpak, V.B. Molodkin, M.V. Koval'chuk, V.L. Nosik, A.I. Nizkova, V.F. Machulin, I.V. Prokopenko, E.N. Kislovskiy, V.P. Klad'ko, S.V. Dmitriev, E.V. Pervak, E.G. Len, A.A. Belotskaya, Ya.V. Vasilik, A.I. Grankina, I.N. Zabolotnyy, A.A. Katasonov, M.T. Kogut, O.S. Kononenko, A.V. Mel'nik, V.V. Molodkin, L.I. Ninichuk, I.I. Rudnitskaya, and B.F. Zhuravlev, *Metallofiz. Noveishie Tekhnol.*, **31**, No. 8: 1041 (2009) (in Russian).
43. S.M. Brovchuk, V.B. Molodkin, A.I. Nizkova, I.I. Rudnytska, G.I. Grankina, V.V. Lizunov, S.V. Lizunova, B.V. Sheludchenko, E.S. Skakunova, S.V. Dmitriev, I.N. Zabolotnyi, A.A. Katasonov, B.F. Zhuravlev, R.V. Lekhnyak, L.N. Skapa, and N.P. Irha, *Metallofiz. Noveishie Tekhnol.*, **36**, No. 8: 1035 (2014). https://doi.org/10.15407/mfint.36.08.1035
44. V.V. Lizunov, S.M. Brovchuk, A.I. Nizkova, V.B. Molodkin, S.V. Lizunova, B.V. Sheludchenko, A.I. Grankina, I.I. Rudnitskaya, S.V. Dmitriev, N.G. Tolmachev, R.V. Lekhnyak, L.N. Skapa, N.P. Irkha, *Metallofiz. Noveishie Tekhnol.*, **36**, No. 9: 1271 (2014) (in Russian). https://doi.org/10.15407/mfint.36.09.1271
45. V.B. Molodkin, A.I. Nizkova, V.V. Lizunov, V.V. Molodkin, E.N. Kislovskiy, Ya.V. Vasilik, O.V. Reshetnik, T.P. Vladimirova, A.A. Belotskaya, and N.V. Barvinok, *Metallofiz. Noveishie Tekhnol.*, **40**, No. 8: 1123 (2018) (in Russian). https://doi.org/10.15407/mfint.40.08.1123
46. A.P. Shpak, V.B. Molodkin, M.V. Koval'chuk, V.L. Nosik, A.I. Nizkova, V.F. Machulin, I.V. Prokopenko, E.N. Kislovskiy, V.P. Klad'ko, S.V. Dmitriev, E.V. Pervak, E.G. Len, A.A. Belotskaya, Ya.V. Vasilik, A.I. Grankina, I.N. Zabolotnyy, A.A. Katasonov, M.T. Kogut, O.S. Kononenko, A.V. Mel'nik, V.V. Molodkin, L.I. Ninichuk, and I.I. Rudnitskaya, *Metallofiz. Noveishie Tekhnol.*, **31**, No. 7: 927 (2009) (in Russian).
47. V.B. Molodkin, H.I. Nizkova, Ye.I. Bogdanov, S.I. Olikhovskii, S.V. Dmitriev, M.G. Tolmachev, V.V. Lizunov, Ya.V. Vasylyk, A.G. Karpov, and O.G. Voytok, *Usp. Fiz. Met.*, **18**, No. 2: 177 (2017) (in Ukrainian). https://doi.org/10.15407/ufm.18.02.177

48. V.V. Nemoshkalenko, V.B. Molodkin, E.N. Kislovskiy, S.I. Olikhovskiy, T.A. Grishchenko, M.T. Kogut, and E.V. Pervak, *Metallofiz. Noveishie Tekhnol.*, **22**, No. 2: 42 (2000) (in Russian).
49. V.V. Nemoshkalenko, V.B. Molodkin, S.I. Olikhovskiy, E.N. Kislovskiy, M.T. Kogut, L.M. Sheludchenko, and E.V. Pervak, *Metallofiz. Noveishie Tekhnol.*, **22**, No. 2: 51 (2000) (in Russian).

Received September 14, 2018;
in final version, December 3, 2018

В.В. Лізунов, І.М. Заболотний,
Я.В. Василик, І.Е. Голентус, М.В. Ушаков
Інститут металофізики ім. Г.В. Курдюмова НАН України,
бульв. Акад. Вернадського, 36, 03142 Київ, Україна

ІНТЕГРАЛЬНА ДИФРАКТОМЕТРІЯ:
ДОСЯГНУТІ УСПІХИ ТА НОВІ МОЖЛИВОСТІ

Статтю присвячено обговоренню динамічної інтегральної дифрактометрії та її функціональних можливостей. Показано, що комбіноване використання вимірювань інтегральних дифракційних параметрів за різних умов дифракції уможливлює визначення параметрыв мікродефектів декількох типів, одночасно присутніх у монокристалі. Обговорюються приклади використання вимірювання повної інтегральної інтенсивности динамічної дифракції, внеску її дифузійної складової та їхніх залежностей від різних умов динамічної дифракції для неруйнівної експресної діагностики характеристик дефектної структури монокристалічних систем.

Ключові слова: динамічна дифракція, дифузне розсіяння, інтегральна дифрактометрія, мікродефекти.

В.В. Лизунов, И.Н. Заболотный,
Я.В. Василик, И.Э. Голентус, Н.В. Ушаков
Институт металлофизики им. Г.В. Курдюмова НАН Украины,
бульв. Акад. Вернадского, 36, 03142 Киев, Украина

ИНТЕГРАЛЬНАЯ ДИФРАКТОМЕТРИЯ:
ДОСТИГНУТЫЕ УСПЕХИ И НОВЫЕ ВОЗМОЖНОСТИ

Статья посвящена обсуждению динамической интегральной дифрактометрии и её функциональных возможностей. Показано, что комбинированное использование измерений интегральных дифракционных параметров при различных условиях дифракции позволяет определять параметры микродефектов нескольких типов, одновременно присутствующих в монокристалле. Обсуждаются примеры использования измерения полной интегральной интенсивности динамической дифракции, вклада её диффузной составляющей и их зависимостей от различных условий динамической дифракции для неразрушающей экспрессной диагностики характеристик дефектной структуры монокристалличе-ских систем.

Ключевые слова: динамическая дифракция, диффузное рассеяние, интегральная дифрактометрия, микродефекты.